

Spectrum of SU(2) gauge theory at large number of flavors

Jarno Rantaharju,^{*} Tobias Rindlisbacher,[†] Kari Rummukainen,[‡] Ahmed Salami,[§] and Kimmo Tuominen[¶]
Department of Physics & Helsinki Institute of Physics, P.O. Box 64, FI-00014 University of Helsinki

We present a numerical study of the spectrum of an asymptotically non-free SU(2) gauge theory with $N_f = 24$ massive fermion flavors. For such large number of flavors, asymptotic freedom is lost and the massless theory is governed by a gaussian fixed point at long distances. If fermions are massive they decouple at low energy scales and the theory is confining. We present a scaling law for the masses of the hadrons, glueballs and string tension as functions of fermion mass. The hadrons become effectively heavy quark systems, with masses approximately twice the fermion mass, whereas the energy scale of the confinement, probed by e.g. the string tension, is much smaller and vanishes asymptotically as $m_{\text{fermion}}^{2.18}$. Our results from lattice simulations are compatible with this behaviour.

I. INTRODUCTION

Asymptotically free nonabelian gauge-fermion theories are a cornerstone of our theoretical understanding of the elementary particle interactions of ordinary matter. The first principle methodologies of lattice field theory to solve these theories where perturbative methods are inapplicable are well established. Recently much effort has been devoted to studies of gauge-fermion theories whose matter content facilitates the existence of an infrared fixed point [1] as such theories are of interest for beyond standard model phenomenology [2–4]. On the lattice the properties of this type of theories have been studied for SU(2) gauge theory with matter fields in the fundamental [5–9] or adjoint [10–18] representation. For related studies in SU(3) case, see e.g. [19–25] for fundamental representation fermions and [26–30] for two-index symmetric representation. Analyses have been extended also to SU(4) gauge group with fermions in fundamental and higher representations [31, 32].

However, less is known of the precise dynamics of gauge theories with many fermion flavors so that the theory is no longer asymptotically free. While such a particle content is not directly relevant for the Standard Model of elementary particle interactions, it poses an interesting challenge for general understanding of gauge theory dynamics on one hand and on the development of computational methods on the other.

Broadly, the non-asymptotically free theories can be categorized as trivial or asymptotically safe. The former means that the theory develops an ultraviolet (UV) cutoff and can be interpreted consistently as a fundamental theory only as a free theory at short distances, while the latter means that a non-perturbative UV fixed point emerges and controls the short distance behavior of the theory.

In an earlier study [33], we analysed this question in SU(2) gauge theory with 24 and 48 massless Dirac fermions by measuring the evolution of the coupling con-

stant. Our results suggested that SU(2) gauge theory at these large numbers of fermions does not have an UV fixed point but is in the category of trivial theories. The results on the running coupling were seen to match well with the perturbative running in the infrared (IR).

In this paper we continue the lattice investigation of SU(2) gauge theory with 24 flavors. The aim is to complement our earlier results on the measurement of the coupling by a computation of the spectrum of the theory, i.e. the determination of long distance or infrared (IR) behavior, as the quark¹ mass m_q is varied. When the quark mass is non-vanishing the infrared behaviour of the theory changes: at energy scales smaller than the quark mass m_q , the quarks decouple and the physics is effectively that of confining SU(2) gauge theory with heavy quarks. The spectrum of the theory includes two quark baryons, quark-antiquark mesons and glueballs, and the string tension is non-vanishing. In terms of the renormalization group (RG) flow, the point ($g^2 = 0, m_q = 0$) is an infrared fixed point, and g^2 and m_q are irrelevant and relevant parameters, respectively.

We introduce scaling laws for the hadron masses and quantities probing confinement (string tension, glueballs) as the quark mass is reduced. Our main result is that the hadrons behave as heavy quark systems, with masses close to $2m_q$, whereas the energy scale characterizing confinement is much smaller, and asymptotically vanishes proportional to $m_q^{2.18}$. Our lattice measurements agree with these predictions, although the confinement scale turns out to be so small that we can only give upper limits to it. Together with our earlier work, the present paper establishes a consistent picture for the nonperturbative behaviors in this theory from IR to UV scales.

The paper is organized as follows: in Section II we introduce the expected scaling of the relevant mass scales of the theory. In Section III we briefly describe the lattice formulation and in Section IV we describe the lattice measurements and the results. In Section V we conclude and outline possibilities for further work.

^{*} jarno.rantaharju@helsinki.fi

[†] tobias.rindlisbacher@helsinki.fi

[‡] kari.rummukainen@helsinki.fi

[§] ahmed.salami@helsinki.fi

[¶] kimmo.i.tuominen@helsinki.fi

¹ For concreteness, we call the fermions “quarks”.

II. EXPECTED MASS SPECTRUM

The solution of the 1-loop β -function for SU(2) gauge theory with N_f massless quarks is

$$g^2(\mu) = \frac{1}{2\beta_0^{(N_f)} \log(\mu/\Lambda)}. \quad (1)$$

Let us consider the case $N_f = 24$. Now $\Lambda = \Lambda_{UV}$ is the UV Landau pole, $\mu < \Lambda_{UV}$ and $\beta_0^{(24)} \approx -0.0549$. Thus, when the energy scale $\mu \rightarrow 0$ the coupling constant g^2 vanishes, and the system is free in the infrared: there are no bound states, and the string tension vanishes.

However, if the quarks are massive the situation changes dramatically: when $\mu \ll m_q$, the quarks decouple and the system effectively becomes confining pure gauge SU(2) theory. String tension is non-vanishing, and the mass spectrum includes glueballs, quark-antiquark mesons and two-quark baryons.

The energy scale of the confinement of SU(2) gauge theory sets the mass scale of glueballs and string tension. We can make a rough estimate of the confinement scale with the 1-loop running of the coupling in $N_f = 24$ and $N_f = 0$ theories, and setting the couplings equal at $\mu = m_q$:

$$g^2(\mu = m_q, N_f = 24) = g^2(\mu = m_q, N_f = 0). \quad (2)$$

Let us call the Λ -parameter of the $N_f = 0$ theory Λ_{IR} . It is analogous to “ Λ_{QCD} ” of the pure gauge theory and is a proxy for the confinement energy scale. Alternatively, we could use a fixed large value of $g^2(\mu)$ to set the scale, and conclusions would remain unchanged.

Solving for Λ_{IR} in terms of the quark mass and the UV scale Λ_{UV} we obtain

$$\frac{\Lambda_{IR}}{\Lambda_{UV}} = \left(\frac{m_q}{\Lambda_{UV}} \right)^{1 - \beta_0^{(24)}/\beta_0^{(0)}} \approx \left(\frac{m_q}{\Lambda_{UV}} \right)^{2.18}. \quad (3)$$

Thus, the confinement scale, and hence the glueball masses and the square root of the string tension, are proportional to $m_q^{2.18}$ at small quark masses. While the approximation (3) is based on 1-loop running and an abrupt mass threshold, it should become accurate in the limit $m_q/\Lambda_{UV} \rightarrow 0$ because the coupling near $\mu = m_q$ will be small, and the small coupling region dominates the evolution of the scale.

On the other hand, because $m_q/\Lambda_{IR} \gtrsim 1$ and grows as m_q decreases, the 2-quark hadrons are effectively “heavy quark” systems, with masses

$$m_{\text{Hadron}} \approx 2m_q. \quad (4)$$

The size of the heavy quark system is proportional to its “Bohr radius”, $[m_q g^2(m_q)]^{-1}$.

A more accurate estimation of the confinement scale can be obtained with the massive 2-loop β -function [34]. In this case the mass threshold is automatically taken care by the β and γ -functions:

$$\mu \frac{dg^2}{d\mu} = \beta(g^2, m_q/\mu), \quad (5a)$$

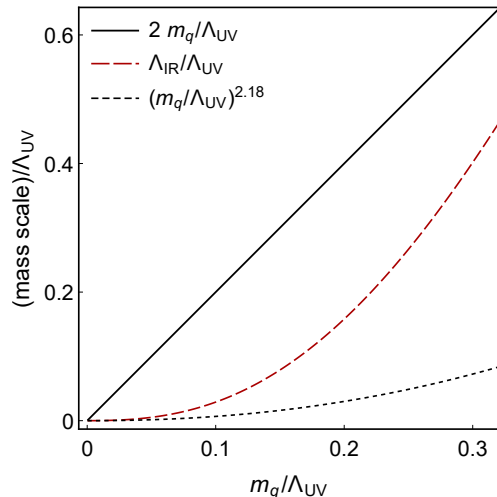


Figure 1. The expected scaling of meson/baryon masses $m_{\text{Hadron}} \approx 2m_q$ and the confinement scale Λ_{IR} , which is proportional to the glueball masses and square root of the string tension, as functions of quark mass m_q . The long-dashed, red line is obtained using the 2-loop massive quark β -function (5b) and the short-dashed, black line is the approximation (3).

$$\frac{\mu}{m_q} \frac{dm_q}{d\mu} = -\gamma(g^2, m_q/\mu). \quad (5b)$$

Because also quark mass is running, we set the physical quark mass at the initial scale $\mu_0 = 2m_{q,0}$, give a range of initial values to $g^2(\mu_0)$ and evolve the equations to UV and IR until the coupling diverges. The result $\Lambda_{IR}/\Lambda_{UV}$ is shown in Fig. 1 as functions of $m_{q,0}/\Lambda_{UV}$. We observe that this result agrees with the approximation (3) at small m_q , but deviates from it substantially at larger m_q when the mass threshold effects and higher order corrections affect the result significantly. Our goal is to observe how well this behaviour is reproduced on the lattice.

III. LATTICE FORMULATION

On the lattice the theory is defined by the action

$$S = S_G(U) + S_F(V) + c_{SW} S_{SW}(V), \quad (6)$$

where U is a SU(2) gauge link matrix in the fundamental representation, V is a corresponding smeared gauge link, defined by hypercubic truncated stout smearing (HEX smearing) [35], S_G is the Wilson gauge action, and S_F and S_{SW} are, respectively, the Wilson fermion action and the clover term. The parameters of the action are the bare lattice gauge coupling $\beta_L \equiv 4/g_0^2$, appearing in S_G , the “hopping parameter” κ in S_F , and the Sheikholeslami-Wohlert coefficient c_{SW} . We set $c_{SW} = 1$, as is often used for HEX smeared fermions [17].

We simulate $N_f = 24$ massive but mass-degenerate Wilson flavors on hyper-cubic, toroidal lattices of sizes $V = N_s^3 \times N_t$, where N_s and N_t refer to the number of lattice sites in spatial and temporal direction. These cover the

values $N_t \in \{32, 40, 48\}$ and $N_s \in \{N_t/2, 3N_t/4, N_t\}$. The boundary conditions for the gauge field are periodic in all directions, whereas for the fermion fields, they are periodic only in spatial but anti-periodic in temporal direction, as usual.

Simulations are carried out using a hybrid Monte Carlo (HMC) algorithm with leapfrog integrator and chronological initial values for the fermion matrix inversion [36]. The HMC trajectories have unit-length and the number of leapfrog steps is tuned to yield acceptance rates above 80% (with a few exceptions).

The physical quark mass is determined by the lattice PCAC relation

$$a m_q(x_4) = \frac{(\partial_4^* + \partial_4) f_A(x_4)}{4 f_P(x_4)}, \quad (7)$$

where ∂_4 and ∂_4^* are, respectively, forward and backward lattice time-derivative operators, and

$$f_A(x_4) = -\frac{1}{N_s^3 N_t} \sum_{\mathbf{x}, \mathbf{y}, a} \langle A_\mu^a(\mathbf{y}, y_4) A_\mu^a(\mathbf{x}, x_4 + y_4) \rangle,$$

$$f_P(x_4) = \frac{1}{N_s^3 N_t} \sum_{\mathbf{x}, \mathbf{y}, a} \langle P^a(\mathbf{y}, y_4) P^a(\mathbf{x}, x_4 + y_4) \rangle$$

are the axial current and pseudoscalar density correlation functions with point sources:

$$A_\mu^a(x) = \bar{\psi}(x) \gamma_\mu \gamma_5 \frac{1}{2} \tau^a \psi(x),$$

$$P^a(x) = \bar{\psi}(x) \gamma_5 \frac{1}{2} \tau^a \psi(x).$$

For each value of the bare gauge coupling $\beta_L \equiv 4/g_0^2$ the hopping parameter κ in the Wilson fermion action is tuned to cover a range of PCAC fermion masses for which we study the behavior of the spectrum from the chiral limit to heavy quarks. The masses of color singlet meson states are then determined by fitting the time sliced average correlation functions with Coulomb gauge fixed wall sources:

$${}^{(w)}\Gamma^a(x_4) = \sum_{\mathbf{x}, \mathbf{y}} \bar{\psi}(\mathbf{x}, x_4) \Gamma \frac{1}{2} \tau^a \psi(\mathbf{y}, x_4),$$

with Γ representing an element of the Dirac algebra.

IV. RESULTS

Let us now turn to the details of the simulations and the results we have obtained on the spectrum of physical states. The simulation parameters and corresponding PCAC quark masses, pseudoscalar ("π") and vector ("ρ") meson masses together with the acceptance rates and accumulated statistic are given in Appendix A in tables II–IX.

Phase diagram: For the bare gauge coupling we use values $\beta_L = 4/g_0^2 \in \{-0.25, 0.001, 0.25\}$. The small values of β_L might at first seem to imply that the gauge field is deep in an unphysical strong coupling "bulk phase". This is, however, in general not the case, as the Wilson

N_t	N_s	β_L	κ_{cr}	κ_{bulk}
32	32	-0.25	0.131327(4)	0.1215(12)
32	32	0.001	0.130296(2)	0.1186(12)
32	32	0.25	0.129297(2)	0.1140(10)

Table I. The table lists for a system of size $V = N_s^3 \times N_t$ with $N_s = N_t = 32$ and different β -values the values of κ_{cr} and κ_{bulk} , being, respectively, the values of κ for which the PCAC quark mass m_q vanishes, and at which the bulk transition occurs.

fermions induce an effective positive shift in β_L [37, 38]. This is to leading order proportional to the number of flavors and therefore substantial for $N_f = 24$. Indeed, the above values of β_L were successfully used in the measurement of the coupling constant evolution at vanishing fermion masses [33]. A similar effect has been reported in [39] for staggered fermions.

The value of the β_L affects the lattice spacing, but to the opposite direction to lattice QCD: lattice spacing is made smaller when β_L is decreased. Because of the Landau pole the theory on the lattice does not have a continuum limit.

In Fig. 2(a) we show the measured PCAC quark masses m_q as functions of the hopping parameter κ . It is evident that the system has an abrupt phase transition into unphysical "bulk phase" at small values of κ . The approximate location of the bulk transition is shown with vertical shaded bands for each value of β_L . On the large- κ side of the transition there is a range of κ -values where m_q decreases from 0.8–0.9 down to 0 as κ is increased (here, and in what follows, dimensionful quantities are given in units of the lattice spacing a , unless specified otherwise). This is the range where physics can be extracted. The bulk transition is also visible in other observables, for example the pseudoscalar mass (Fig. 2(b)) and plaquette expectation value (Fig. 2(c)). As expected, the pseudoscalar mass is close to $2m_q$.

The (β_L, κ) -plane phase diagram is shown in Fig. 2(d). The physically relevant domain is between the bulk transition and the critical line $\kappa_{cr}(\beta_L)$, where $m_q = 0$. The values of the critical $\kappa_{cr}(\beta_L)$ have been obtained by linear extrapolation of the measured $m_q(\kappa)$ at smallest quark masses. The numerical values of κ_{cr} and the bulk transition κ_{bulk} are shown in Table I.

Finite size effects: As discussed in Section II, the size of the hadrons grow as $m_q \rightarrow 0$, and we can expect large finite size effects in this limit. This is evident in Fig. 3(a), where we show the pseudoscalar "pion" masses m_π measured from volumes N_s^3 from 12^3 up to 32^3 at different values of β_L . At small volumes the mass plateaus roughly at $m_\pi \approx 1/(N_s a)$ as m_q is lowered. Interestingly, there is very little dependence on the value of the lattice gauge coupling β_L , indicating that it is the quark mass which is important for finite size effects.

In Fig. 3(b) we show the expectation values of the spatial Polyakov loop $\langle P \rangle$ as functions of the quark mass. A non-zero value indicates that the system becomes spatially deconfined, i.e. the volume is too small to contain the confinement physics. The negative expectation value is due to the periodic boundary conditions for fermions to

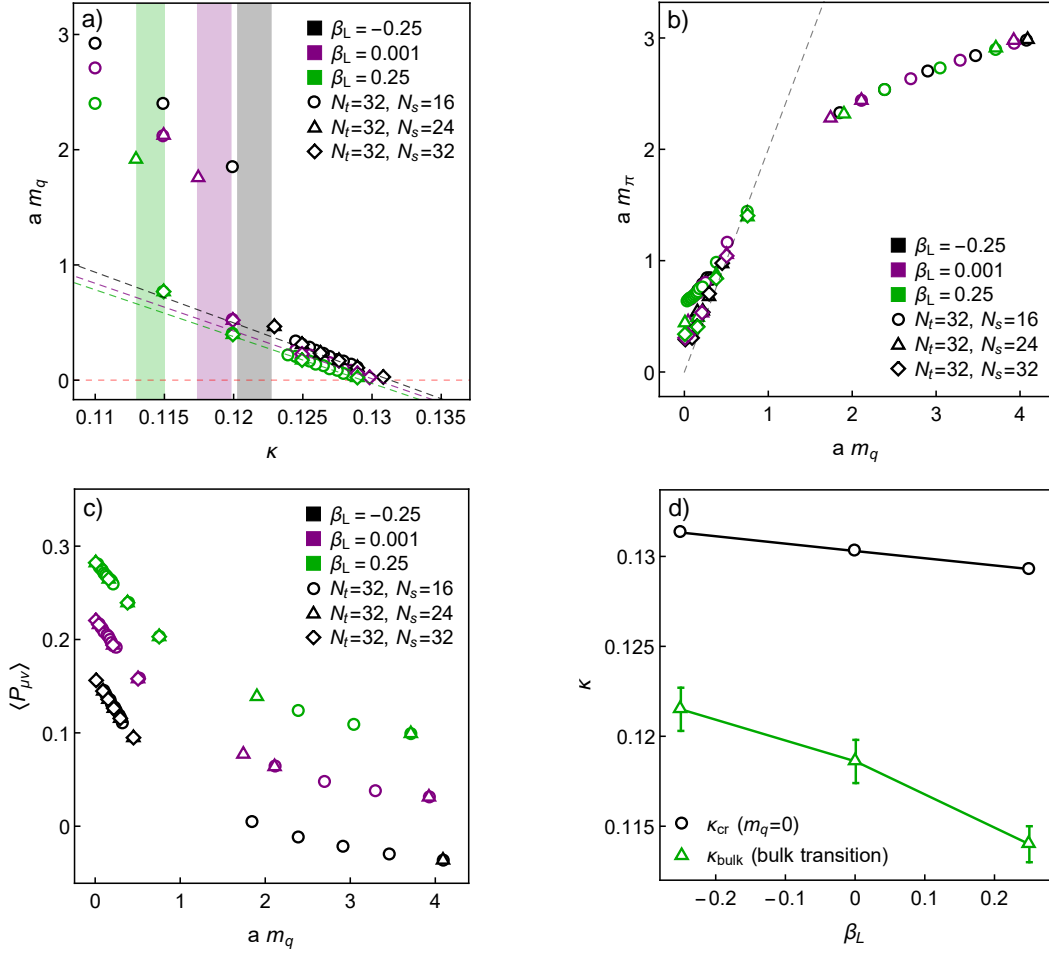


Figure 2. (a): The PCAC quark masses m_q as functions of κ , measured at $\beta_L = -0.25, 0.001, 0.25$ and lattice sizes $V = N_s^3 \times N_t$ with $N_t = 32, N_s = 16, 24, 32$. Here, and in what follows, different colours indicate the β_L -values and plot symbol shapes the volume. The vertical shaded bands show the approximate locations of the bulk phase transitions at different β_L . The dashed lines are linear fits to three smallest m_q -values for each β_L , used to determine the critical value κ_{cr} . (b): The pseudoscalar meson (“pion”) mass m_π and (c): plaquette as functions of m_q . In (b) the dashed line is $m_\pi = 2m_q$ -line. (d): The phase diagram of the system. The physical domain is between the bulk transition and critical ($m_q = 0$) lines.

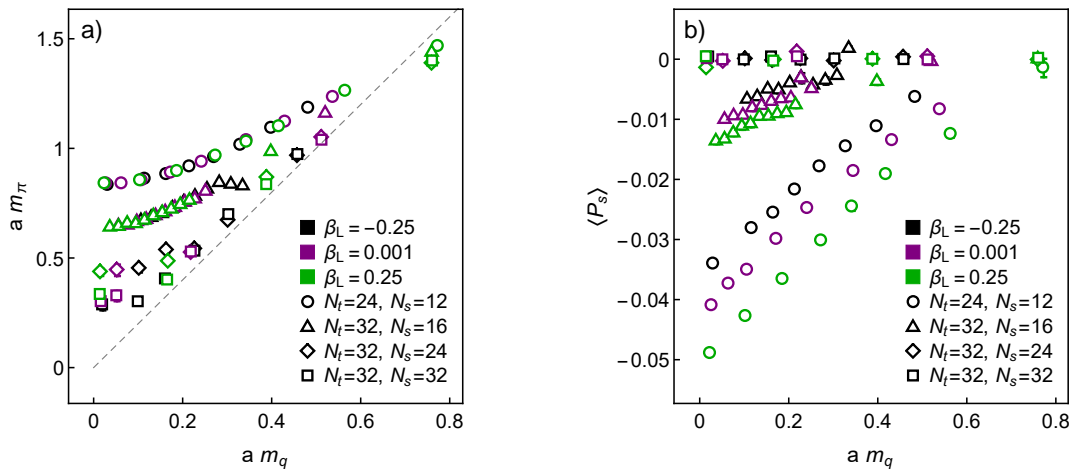


Figure 3. The figure shows for three different values of $\beta_L = -0.25, 0.001, 0.25$ and lattice sizes $V = N_s^3 \times N_t$ with $N_s = 16, 24, 32$ at $N_t = 32$ and $N_s = 12$ at $N_t = 24$ (a) the pion mass m_π and (b) the expectation value of spatial Polyakov loop $\langle P_s \rangle$ as functions of the PCAC quark mass m_q . Note that colors (black, purple, green) are used to distinguish between different values of β_L and symbols (circle, triangle, diamond) are used to distinguish the different system sizes.

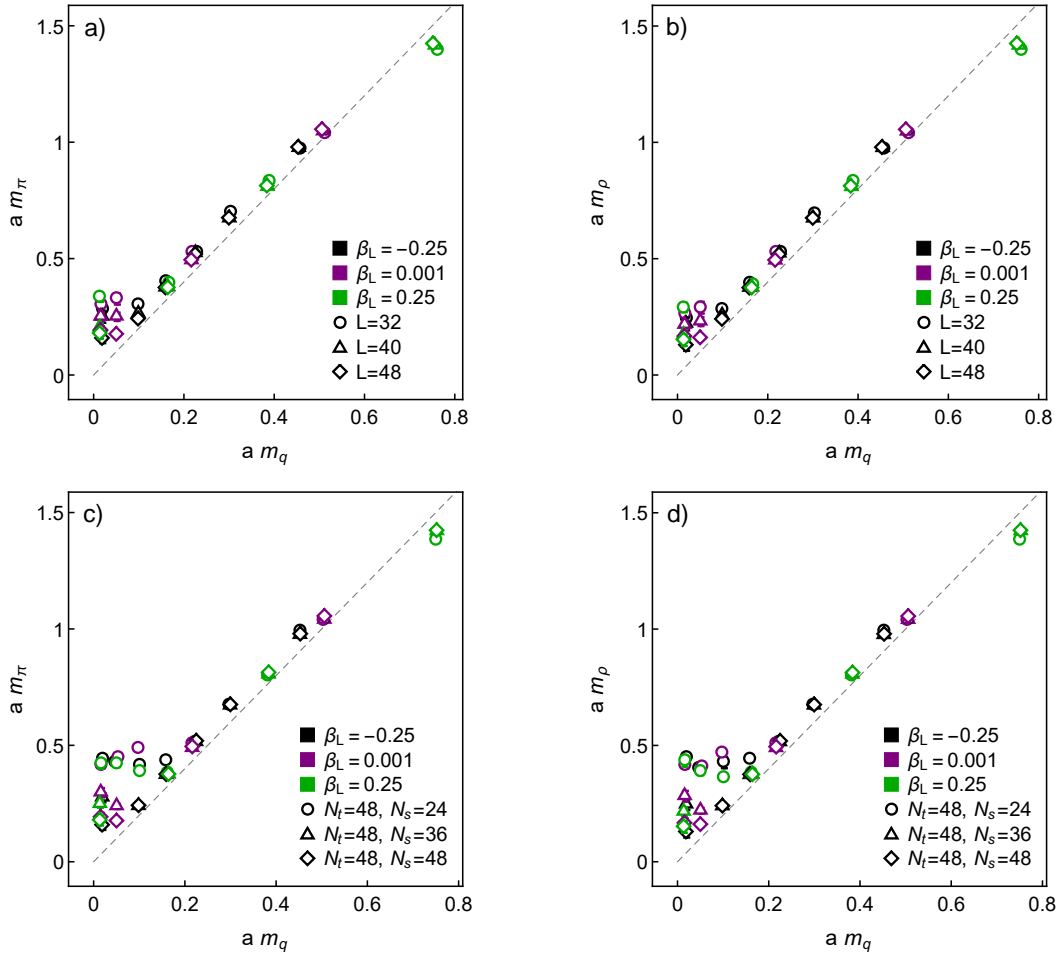


Figure 4. The pseudoscalar meson mass m_π (a,c) and the vector meson mass m_ρ (b,d) as functions of the PCAC quark mass m_q for three values of $\beta_L = -0.25, 0.001, 0.25$ and system sizes $V = N_s^3 \times N_t$, where in (a,b) $N_t = N_s = L$, $L = 32, 40, 48$, and in (c,d) $N_t = 48$, $N_s = 24, 36, 48$. The colours (black, purple, green) are used to distinguish between different values of β_L and symbols (circle, triangle, diamond) are used to distinguish the different system sizes.

spatial directions. Clearly, at small volumes the magnitude of the expectation value of the Polyakov lines grow as the quark mass is decreased. The magnitude of $\langle P \rangle$ is expected to decrease exponentially with the length of the line, N_s . Nevertheless, the behaviour changes qualitatively as the volume is increased: $\langle P \rangle$ remains zero down to progressively smaller values of m_q . At $N_s = 32$ $\langle P \rangle$ remains zero at all m_q , within our statistical accuracy.

Meson spectrum: The spectrum of pseudoscalar and vector mesons is shown in detail in Fig. 4 for the range of m_q away from the bulk phase as discussed above. The pion masses as a function of the quark mass are shown on panels a) and c), and the vector meson on panels b) and d). The results corresponding to β_L values $-0.25, 0.001$ and 0.25 are shown and different values are indicated by colors black, blue and red respectively. In a) and b) the results are shown for system sizes $N_t = N_s = L$ with $L = 32$ (circles), $L = 40$ (triangles) and $L = 48$ (diamonds), while in c) and d) the results are shown for $N_t = 48$ with $N_s = 24$ (circles), $N_s = 36$ (triangles) and $N_s = 48$ (diamonds). Both the quark mass m_q and the hadron masses are in units

of the inverse lattice spacing.

As expected, the hadron masses very closely follow $2m_q$ -line, slightly above it, and significant deviations appear only when $m_{\text{hadron}} \lesssim 1/L$, the inverse spatial size of the lattice. There is also no significant difference between pseudoscalar and vector mesons within the accuracy of our measurements. This demonstrates the heavy quark nature of the mesons.

The results are independent of the bare lattice coupling β_L in the sense that the results fall on a universal line on the (m_q, m_{Hadron}) -plane. We remind the reader that the lattice spacing becomes smaller as β_L is decreased (bare coupling grows when lattice spacing is decreased), but the theory has no continuum limit because of the UV Landau pole. Nevertheless, the observed universal behaviour in β_L indicates that the theory has a scaling window where continuum-like physics can be studied.

String tension and glueballs: In Section II it was predicted that the confinement scale, which determines the string tension and the glueball masses, scale as $(m_q/\Lambda_{\text{UV}})^{2.18}$ at small m_q , with deviations expected at

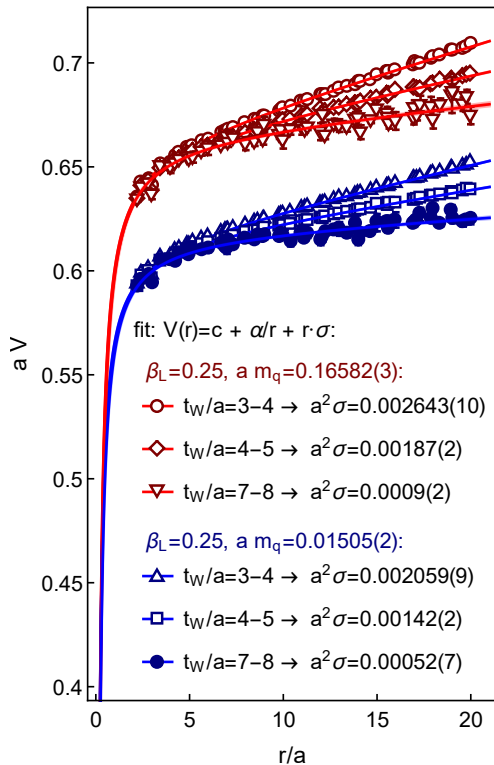


Figure 5. Examples of fitting the effective potential while the t -distance of the Wilson loops, t_w , is varied. The result does not settle to an asymptotic value, and the result is only an upper bound.

larger m_q (see Fig. 1). We measure the string tension σ by constructing Wilson loops using spatially smeared gauge fields, with 5 different APE smearing levels up to 32 smearings [40]. We measure Wilson loops $W(\mathbf{r}, t)$, where \mathbf{r} is an integer multiple of one of the spatial vectors $(1, 0, 0)$, $(1, 1, 0)$, $(1, 1, 1)$, $(2, 1, 0)$, $(2, 1, 1)$ + reflections and permutations. The large- t behaviour of the Wilson loops is fitted with an effective potential

$$\log \frac{W(\mathbf{r}, t+1)}{W(\mathbf{r}, t)} = \frac{A}{r} + \sigma r + B, \quad (8)$$

where $r = |\mathbf{r}|$ and A , B and σ are fit parameters.

However, it turns out that the string tension is too small in order to be reliably measured using our lattice sizes and statistics. We can only present upper limits for the string tension, measured from the largest t -distance before the statistical errors make the measurement meaningless. Nevertheless, the measurements have not yet stabilized as t is changed. This is shown in Fig. 5. We also attempted to do generalized eigenvalue analysis of the Wilson loops between different smearing levels, but this did not stabilize either, presumably because the spacing between eigenvalues is too small.

The upper limits of the square root of string tension are shown in Fig. 6. To guide the expectation, the simple scaling ansatz (3) is shown by the dashed line, with arbitrary scaling.

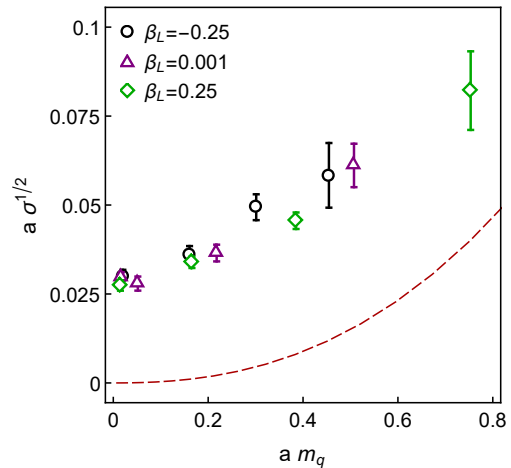


Figure 6. The upper limit of the square root of the string tension $\sigma^{1/2}$ as function of the quark mass m_q . The dashed line shows the confinement scale Λ_{IR} from Fig. 1, assuming (arbitrarily) that $a/\Lambda_{\text{UV}} \sim 24$.

Finally, we attempt to measure glueball correlation functions using spatially smeared gauge links, with up to 100 APE smearing steps. From the smeared gauge fields we construct operators coupling to scalar $J^{PC} = 0^{++}$ and tensor 2^{++} glueballs. On the lattice the operators transform under cubic group representations, and we measure operators under 6 different representations. Considering the difficulties in measuring the string tension, it is perhaps not surprising that we were not able to reliably measure glueball masses. The correlation functions coupling to the 0^{++} state are very noisy due to the disconnected contribution. Correlation functions of operators in the cubic group representations E^{++} and T_2^{++} , which couple to the continuum 2^{++} state, do not have a disconnected part and are somewhat better behaved. Nevertheless, we were not able to obtain the asymptotic state in these channels.

We assign the failure of the glueball mass measurement to the (expected) small value of the masses. This implies that the numerous excited states coupling to the same operators also have small masses, and it becomes very difficult to find the ground state. We attempted to use generalized eigenvalue analysis of operators with different number of smearing steps, but the small mass gaps between states rendered the procedure unstable.

In Fig. 7 we plot together the pseudoscalar mass and the upper limit of the square root of the string tension, measured from 48^4 lattices. m_π is more than an order of magnitude larger than the upper limit of $\sigma^{1/2}$, and at the smaller end of the m_π -range the true hierarchy is expected to become much larger. Comparing with Fig. 1, we can conclude that the physics on our lattices correspond to the case where quark masses are substantially below the Landau pole, $m_q/\Lambda_{\text{UV}} \ll 1$. Because in the lattice units $m_q a \lesssim 1$, this implies that the Landau pole is effectively at considerably larger scale than the inverse lattice spacing, $\Lambda_{\text{UV}} \gg 1/a$. This was also observed in our earlier study of the running coupling at massless theory [33].

It is difficult to reach larger values of m_q/Λ_{UV} with lattice simulations: trying to make the bare coupling stronger and the quarks heavier moves us towards the direction of strong lattice artifacts. With our choice of the lattice action the bulk transition prevents us from using heavier quarks.

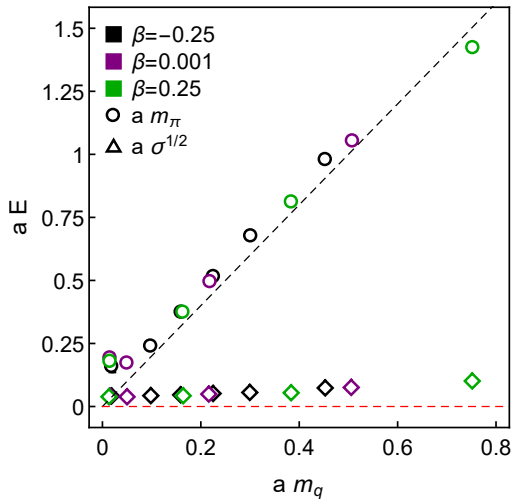


Figure 7. The pseudoscalar mass m_π and the upper limit of the square root of string tension $\sigma^{1/2}$ as functions of m_q . The data is measured from lattices of size 48^4 .

V. CONCLUSIONS

We have studied the mass spectrum of SU(2) gauge theory with $N_f = 24$ Dirac fermions on the lattice, complementing our earlier analysis [33] on the running coupling in this theory. The massless theory is free in the infrared, without bound states. When the quark mass m_q is non-zero the behaviour is different: in the infrared the theory is confining, and its spectrum includes mesons, two-quark baryons and glueballs, and the string tension is non-vanishing. We have presented scaling relations for the hadron masses and for the confinement scale as functions of the quark mass. The hadrons behave effectively as heavy quark systems with masses close to $2m_q$, whereas the confinement scale decreases faster, at small m_q proportional to $m_q^{2.18}$.

The scaling relations imply that glueball masses and square root of the string tension $\sigma^{1/2}$ are much smaller than hadron masses unless quarks are very heavy, with masses of the order of the Landau pole of the theory. The results from lattice simulations confirm this behaviour: $\sigma^{1/2}$ is more than an order of magnitude smaller than the hadron masses. However, we were only able to give an upper limit for $\sigma^{1/2}$ in the range of quark masses studied, and we expect the true result to be substantially below the upper limit at small m_q .

To fully verify the behaviour of the confinement scale as m_q is varied we would need to use much heavier quarks and stronger lattice coupling, so that the quark mass should be close to the Landau pole, $m_q/\Lambda_{UV} \lesssim 1$. However, lat-

tice bulk transition and increased lattice artifacts prevent us from moving significantly to that direction. Furthermore, because the theory is only defined up to the UV cutoff scale, moving quark masses close to it makes the relevant physics sensitive to the details of the UV regularization used.

VI. ACKNOWLEDGEMENT

The support of the Academy of Finland grants 308791, 310130, 319066 and 320123 is acknowledged. The authors wish to acknowledge CSC - IT Center for Science, Finland, for generous computational resources.

Appendix A: Tables of simulation parameters and results

A summary of the simulation parameters and corresponding PCAC quark masses, pion and rho-meson masses, as well as the acceptance rates and accumulated statistics (after subtraction of non-thermalized configurations), is given in the tables II–IX.

N_t	N_s	β_L	κ	m_q	m_π	m_ρ	acc.	stat.
24	12	-0.25	0.1309	0.037(2)	0.84(5)	0.91(5)	0.98	8.8k
24	12	-0.25	0.129	0.133(5)	0.79(5)	0.80(7)	0.98	9k
24	12	-0.25	0.128	0.194(5)	0.86(3)	0.87(4)	0.99	9.3k
24	12	-0.25	0.127	0.263(5)	0.91(3)	0.93(3)	0.99	9.5k
24	12	-0.25	0.126	0.337(8)	0.98(4)	0.99(4)	0.99	9.7k
24	12	-0.25	0.125	0.40(2)	1.00(4)	1.00(5)	0.99	9.7k
24	12	-0.25	0.124	0.49(2)	1.08(3)	1.09(4)	0.99	9.5k
24	12	-0.25	0.123	0.58(2)	1.13(3)	1.14(3)	0.99	9.8k
24	12	0.001	0.1299	0.029(1)	0.77(4)	0.76(6)	0.99	9.2k
24	12	0.001	0.129	0.077(3)	0.86(4)	0.88(5)	0.99	9.4k
24	12	0.001	0.128	0.129(3)	0.85(3)	0.84(4)	0.99	9.5k
24	12	0.001	0.1265	0.202(6)	0.85(4)	0.87(4)	0.99	9.5k
24	12	0.001	0.125	0.288(9)	0.93(4)	0.95(4)	0.99	9.6k
24	12	0.001	0.123	0.411(8)	1.03(3)	1.03(3)	0.99	10.2k
24	12	0.001	0.1215	0.50(2)	1.06(3)	1.07(3)	0.99	10.1k
24	12	0.001	0.12	0.66(1)	1.22(2)	1.22(2)	0.99	10.2k
24	12	0.25	0.129	0.0270(8)	0.81(4)	0.79(5)	0.99	9.6k
24	12	0.25	0.127	0.121(3)	0.82(3)	0.85(4)	0.99	9.9k
24	12	0.25	0.125	0.231(6)	0.93(3)	0.96(3)	0.99	10.1k
24	12	0.25	0.123	0.33(1)	0.98(4)	0.99(4)	0.99	10.6k
24	12	0.25	0.1215	0.392(9)	0.98(4)	1.00(4)	0.99	10.5k
24	12	0.25	0.12	0.50(1)	1.10(3)	1.11(3)	0.99	10.3k
24	12	0.25	0.1175	0.64(2)	1.16(4)	1.16(4)	0.99	6k
24	12	0.25	0.115	0.92(2)	1.41(2)	1.41(2)	0.99	11.5k

Table II. The table shows for systems of size $V = N_s^3 \times N_t$ with $N_t = 24$ and $N_s = 12$ the simulated values of β_L and κ , the corresponding PCAC quark mass, m_q , pion and ρ -meson masses, m_π , m_ρ , the acceptance rate of the HMC trajectories, and the number of usable configurations (after thermalization).

N_t	N_s	β_L	κ	m_q	m_π	m_ρ	acc.	stat.
32	32	-0.25	0.1309	0.0207(2)	0.28(3)	0.24(3)	0.89	0.4k
32	32	-0.25	0.129	0.1008(2)	0.299(5)	0.284(5)	0.84	0.5k
32	32	-0.25	0.1277	0.1619(2)	0.403(6)	0.397(6)	0.84	1.2k
32	32	-0.25	0.1263	0.2282(2)	0.530(2)	0.530(2)	0.84	1.3k
32	32	-0.25	0.125	0.3043(2)	0.697(6)	0.695(7)	0.82	1.5k
32	32	-0.25	0.123	0.4595(5)	0.971(3)	0.971(3)	0.84	1.7k
32	32	0.001	0.1299	0.0176(1)	0.30(2)	0.26(2)	0.89	1.4k
32	32	0.001	0.129	0.0526(1)	0.33(3)	0.29(3)	0.83	0.9k
32	32	0.001	0.125	0.2201(2)	0.53(2)	0.52(2)	0.83	1.4k
32	32	0.001	0.12	0.5136(5)	1.036(2)	1.036(2)	0.85	1.7k
32	32	0.25	0.129	0.0155(1)	0.33(2)	0.29(2)	0.86	0.7k
32	32	0.25	0.125	0.1669(1)	0.398(2)	0.391(2)	0.89	1.1k
32	32	0.25	0.12	0.3894(2)	0.833(5)	0.832(5)	0.88	1.5k
32	32	0.25	0.115	0.762(2)	1.40(2)	1.40(2)	0.88	1.9k

Table III. Same as Table II for $N_t = 32$, $N_s = 32$.

N_t	N_s	β_L	κ	m_q	m_π	m_ρ	acc.	stat.
40	20	-0.25	0.1309	0.0226(1)	0.50(2)	0.50(2)	0.95	2k
40	20	-0.25	0.1302	0.0509(1)	0.48(2)	0.51(2)	0.97	1.3k
40	20	-0.25	0.129	0.1045(2)	0.56(1)	0.54(2)	0.86	1k
40	20	-0.25	0.1277	0.1646(2)	0.51(2)	0.48(2)	0.85	0.6k
40	20	-0.25	0.1263	0.2292(3)	0.64(2)	0.65(2)	0.88	0.3k
40	20	-0.25	0.125	0.2978(5)	0.663(3)	0.663(3)	0.89	0.2k
40	20	-0.25	0.123	0.4538(4)	0.971(4)	0.972(4)	0.86	2k
40	20	0.001	0.1299	0.0189(1)	0.53(2)	0.57(2)	0.97	2k
40	20	0.001	0.129	0.0547(1)	0.52(2)	0.57(2)	0.88	1k
40	20	0.001	0.1278	0.1019(1)	0.56(2)	0.54(2)	0.96	1.4k
40	20	0.001	0.125	0.2223(2)	0.61(2)	0.63(2)	0.91	0.5k
40	20	0.001	0.12	0.5099(5)	1.10(2)	1.10(2)	0.9	1.5k
40	20	0.25	0.129	0.0168(1)	0.48(2)	0.50(3)	0.88	1k
40	20	0.25	0.1281	0.0523(1)	0.51(2)	0.53(3)	0.97	1.4k
40	20	0.25	0.1267	0.1032(1)	0.54(3)	0.57(3)	0.97	0.8k
40	20	0.25	0.125	0.1700(2)	0.55(2)	0.55(2)	0.92	0.8k
40	20	0.25	0.12	0.3823(2)	0.801(2)	0.801(2)	0.91	2k
40	20	0.25	0.115	0.7534(6)	1.373(7)	1.374(7)	0.92	2k

Table IV. Same as Table II for $N_t = 40$, $N_s = 20$.

-
- [1] F. Sannino and K. Tuominen, Phys. Rev. D **71** (2005), 051901 doi:10.1103/PhysRevD.71.051901 [arXiv:hep-ph/0405209 [hep-ph]].
- [2] C. T. Hill and E. H. Simmons, Phys. Rept. **381** (2003), 235-402 [erratum: Phys. Rept. **390** (2004), 553-554] doi:10.1016/S0370-1573(03)00140-6 [arXiv:hep-ph/0203079 [hep-ph]].
- [3] D. D. Dietrich, F. Sannino and K. Tuominen, Phys. Rev. D **72** (2005), 055001 doi:10.1103/PhysRevD.72.055001 [arXiv:hep-ph/0505059 [hep-ph]].
- [4] A. Arbey, G. Cacciapaglia, H. Cai, A. Deandrea, S. Le Corre and F. Sannino, Phys. Rev. D **95** (2017) no.1, 015028 doi:10.1103/PhysRevD.95.015028 [arXiv:1502.04718 [hep-ph]].
- [5] T. Karavirta, J. Rantaharju, K. Rummukainen and K. Tuominen, JHEP **05** (2012), 003 doi:10.1007/JHEP05(2012)003 [arXiv:1111.4104 [hep-lat]].
- [6] V. Leino, J. Rantaharju, T. Rantalaiho, K. Rummukainen, J. M. Suorsa and K. Tuominen, Phys. Rev. D **95** (2017) no.11, 114516 doi:10.1103/PhysRevD.95.114516 [arXiv:1701.04666 [hep-lat]].
- [7] V. Leino, K. Rummukainen, J. M. Suorsa, K. Tuominen and S. Tähtinen, Phys. Rev. D **97** (2018) no.11, 114501 doi:10.1103/PhysRevD.97.114501 [arXiv:1707.04722 [hep-lat]].
- [8] V. Leino, K. Rummukainen and K. Tuominen, Phys. Rev. D **98** (2018) no.5, 054503 doi:10.1103/PhysRevD.98.054503 [arXiv:1804.02319 [hep-lat]].
- [9] A. Amato, V. Leino, K. Rummukainen, K. Tuominen and S. Tähtinen, [arXiv:1806.07154 [hep-lat]].
- [10] A. J. Hietanen, J. Rantaharju, K. Rummukainen and K. Tuominen, JHEP **05** (2009), 025 doi:10.1088/1126-6708/2009/05/025 [arXiv:0812.1467 [hep-lat]].
- [11] A. J. Hietanen, K. Rummukainen and K. Tuominen, Phys. Rev. D **80** (2009), 094504

N_t	N_s	β_L	κ	m_q	m_π	m_ρ	acc.	stat.
40	30	-0.25	0.1309	0.0209(1)	0.32(2)	0.28(2)	0.91	1.9k
40	30	-0.25	0.1302	0.0489(1)	0.40(2)	0.39(2)	0.92	0.8k
40	30	-0.25	0.129	0.1015(2)	0.39(3)	0.38(3)	0.75	0.3k
40	30	-0.25	0.1277	0.1615(2)	0.401(3)	0.396(3)	0.74	0.2k
40	30	-0.25	0.1263	0.2270(2)	0.535(8)	0.535(8)	0.77	1k
40	30	-0.25	0.125	0.3018(2)	0.670(1)	0.670(1)	0.79	2k
40	30	-0.25	0.123	0.4557(6)	0.981(6)	0.981(6)	0.76	2k
40	30	0.001	0.1299	0.0176(1)	0.37(2)	0.38(2)	0.94	1.7k
40	30	0.001	0.129	0.0523(1)	0.32(2)	0.29(2)	0.79	1k
40	30	0.001	0.1278	0.0991(1)	0.40(2)	0.38(2)	0.94	1k
40	30	0.001	0.125	0.2185(2)	0.514(3)	0.509(3)	0.92	0.5k
40	30	0.001	0.12	0.5091(4)	1.040(5)	1.040(5)	0.8	2k
40	30	0.25	0.129	0.0155(1)	0.29(2)	0.25(2)	0.81	1k
40	30	0.25	0.1281	0.0503(1)	0.36(2)	0.34(3)	0.94	0.9k
40	30	0.25	0.1267	0.0994(1)	0.29(1)	0.27(1)	0.94	0.5k
40	30	0.25	0.125	0.1659(2)	0.393(2)	0.387(2)	0.81	0.4k
40	30	0.25	0.115	0.7552(8)	1.398(6)	1.398(6)	0.83	2k

Table V. Same as Table II for $N_t = 40$, $N_s = 30$.

N_t	N_s	β_L	κ	m_q	m_π	m_ρ	acc.	stat.
40	40	-0.25	0.1309	0.0203(1)	0.25(3)	0.22(3)	0.91	0.9k
40	40	-0.25	0.129	0.1005(1)	0.262(1)	0.255(1)	0.88	0.8k
40	40	-0.25	0.1277	0.1610(1)	0.375(1)	0.374(1)	0.88	2k
40	40	-0.25	0.1263	0.2272(1)	0.523(2)	0.521(2)	0.9	2k
40	40	-0.25	0.125	0.3023(2)	0.672(1)	0.672(1)	0.89	2k
40	40	-0.25	0.123	0.4561(5)	0.974(2)	0.975(2)	0.88	2k
40	40	0.001	0.1299	0.0173(1)	0.25(2)	0.21(3)	0.9	0.8k
40	40	0.001	0.129	0.0521(1)	0.25(2)	0.23(2)	0.89	1.1k
40	40	0.001	0.125	0.2184(1)	0.492(1)	0.491(1)	0.9	2k
40	40	0.001	0.12	0.5100(4)	1.046(5)	1.045(5)	0.9	2k
40	40	0.25	0.129	0.0151(1)	0.20(2)	0.17(2)	0.91	0.9k
40	40	0.25	0.125	0.1662(1)	0.377(2)	0.376(2)	0.91	2k
40	40	0.25	0.12	0.3868(2)	0.807(2)	0.807(2)	0.92	2k
40	40	0.25	0.115	0.758(2)	1.41(1)	1.42(1)	0.92	2k

Table VI. Same as Table II for $N_t = 40$, $N_s = 40$.

- doi:10.1103/PhysRevD.80.094504 [arXiv:0904.0864 [hep-lat]].
- [12] L. Del Debbio, A. Patella and C. Pica, Phys. Rev. D **81** (2010), 094503 doi:10.1103/PhysRevD.81.094503 [arXiv:0805.2058 [hep-lat]].
- [13] L. Del Debbio, B. Lucini, A. Patella, C. Pica and A. Rago, Phys. Rev. D **80** (2009), 074507 doi:10.1103/PhysRevD.80.074507 [arXiv:0907.3896 [hep-lat]].
- [14] L. Del Debbio, B. Lucini, A. Patella, C. Pica and A. Rago, Phys. Rev. D **82** (2010), 014509 doi:10.1103/PhysRevD.82.014509 [arXiv:1004.3197 [hep-lat]].
- [15] F. Bursa, L. Del Debbio, D. Henty, E. Kerrane, B. Lucini, A. Patella, C. Pica, T. Pickup and A. Rago, Phys. Rev. D **84** (2011), 034506 doi:10.1103/PhysRevD.84.034506 [arXiv:1104.4301 [hep-lat]].
- [16] T. DeGrand, Y. Shamir and B. Svetitsky, Phys. Rev. D **83** (2011), 074507 doi:10.1103/PhysRevD.83.074507 [arXiv:1102.2843 [hep-lat]].
- [17] J. Rantaharju, T. Rantalaiho, K. Rummukainen and K. Tuominen, Phys. Rev. D **93** (2016) no.9, 094509 doi:10.1103/PhysRevD.93.094509 [arXiv:1510.03335 [hep-lat]].

N_t	N_s	β_L	κ	m_q	m_π	m_ρ	acc.	stat.
48	24	-0.25	0.1309	0.0214(1)	0.44(2)	0.45(2)	0.94	2k
48	24	-0.25	0.1302	0.0497(1)	0.43(2)	0.40(2)	0.95	1.6k
48	24	-0.25	0.129	0.1027(2)	0.41(2)	0.43(3)	0.82	2k
48	24	-0.25	0.1277	0.1608(1)	0.435(7)	0.443(7)	0.81	2k
48	24	-0.25	0.1263	0.2245(1)	0.515(1)	0.516(2)	0.81	2k
48	24	-0.25	0.125	0.2991(3)	0.674(3)	0.674(3)	0.83	2k
48	24	-0.25	0.123	0.4539(4)	0.990(8)	0.990(9)	0.82	2k
48	24	0.001	0.1299	0.0182(1)	0.41(2)	0.42(2)	0.95	2k
48	24	0.001	0.129	0.0535(2)	0.45(2)	0.41(2)	0.84	2k
48	24	0.001	0.1278	0.1003(1)	0.49(1)	0.47(2)	0.95	1.8k
48	24	0.001	0.125	0.2168(2)	0.508(2)	0.505(2)	0.84	2k
48	24	0.001	0.12	0.5063(4)	1.037(5)	1.037(5)	0.85	2k
48	24	0.25	0.129	0.0161(1)	0.42(2)	0.43(3)	0.86	2k
48	24	0.25	0.1281	0.0510(1)	0.42(2)	0.39(2)	0.95	1.8k
48	24	0.25	0.1267	0.1008(2)	0.385(7)	0.362(7)	0.95	1.8k
48	24	0.25	0.125	0.1648(1)	0.382(2)	0.384(2)	0.86	2k
48	24	0.25	0.12	0.3821(2)	0.798(1)	0.798(1)	0.87	2k
48	24	0.25	0.115	0.7508(8)	1.384(8)	1.385(8)	0.89	2k

Table VII. Same as Table II for $N_t = 48$, $N_s = 24$.

N_t	N_s	β_L	κ	m_q	m_π	m_ρ	acc.	stat.
48	36	-0.25	0.1309	0.0205(1)	0.28(2)	0.25(3)	0.88	1k
48	36	-0.25	0.129	0.0999(1)	0.238(1)	0.237(1)	0.89	2k
48	36	-0.25	0.1277	0.1602(1)	0.372(1)	0.372(1)	0.9	2k
48	36	-0.25	0.1263	0.2260(1)	0.513(1)	0.513(1)	0.88	2k
48	36	-0.25	0.125	0.3006(2)	0.670(2)	0.670(2)	0.89	2k
48	36	-0.25	0.123	0.4538(5)	0.973(3)	0.973(3)	0.89	2k
48	36	0.001	0.1299	0.0173(1)	0.30(3)	0.28(3)	0.9	2.4k
48	36	0.001	0.129	0.0520(1)	0.24(2)	0.22(2)	0.91	0.6k
48	36	0.001	0.125	0.2175(1)	0.488(1)	0.487(1)	0.91	2k
48	36	0.001	0.12	0.5073(3)	1.038(3)	1.039(3)	0.91	2k
48	36	0.25	0.129	0.0152(1)	0.25(2)	0.21(2)	0.92	1.6k
48	36	0.25	0.125	0.1653(1)	0.376(1)	0.375(1)	0.91	2k
48	36	0.25	0.12	0.3851(2)	0.803(1)	0.803(1)	0.92	2k
48	36	0.25	0.115	0.754(1)	1.42(2)	1.42(2)	0.92	2k

Table VIII. Same as Table II for $N_t = 48$, $N_s = 36$.

- [18] L. Del Debbio, B. Lucini, A. Patella, C. Pica and A. Rago, Phys. Rev. D **93** (2016) no.5, 054505 doi:10.1103/PhysRevD.93.054505 [arXiv:1512.08242 [hep-lat]].
- [19] Z. Fodor, K. Holland, J. Kuti, D. Negradi, C. Schroeder, K. Holland, J. Kuti, D. Negradi and C. Schroeder, Phys. Lett. B **703** (2011), 348-358 doi:10.1016/j.physletb.2011.07.037 [arXiv:1104.3124 [hep-lat]].
- [20] A. Hasenfratz, D. Schaich and A. Veermala, JHEP **06** (2015), 143 doi:10.1007/JHEP06(2015)143 [arXiv:1410.5886 [hep-lat]].
- [21] Z. Fodor, K. Holland, J. Kuti, S. Mondal, D. Negradi and C. H. Wong, JHEP **06** (2015), 019 doi:10.1007/JHEP06(2015)019 [arXiv:1503.01132 [hep-lat]].
- [22] Z. Fodor, K. Holland, J. Kuti, D. Negradi and C. H. Wong, Phys. Lett. B **779** (2018), 230-236 doi:10.1016/j.physletb.2018.02.008 [arXiv:1710.09262 [hep-lat]].
- [23] T. Appelquist *et al.* [Lattice Strong Dynamics], Phys. Rev. D **99** (2019) no.1, 014509 doi:10.1103/PhysRevD.99.014509 [arXiv:1807.08411 [hep-lat]].

N_t	N_s	β_L	κ	m_q	m_π	m_ρ	acc.	stat.
48	48	-0.25	0.1309	0.0202(1)	0.16(2)	0.13(3)	0.92	1.4k
48	48	-0.25	0.129	0.1001(1)	0.239(1)	0.238(1)	0.91	2.9k
48	48	-0.25	0.1277	0.1608(1)	0.373(1)	0.372(1)	0.9	3k
48	48	-0.25	0.1263	0.2266(1)	0.516(1)	0.516(1)	0.91	3.2k
48	48	-0.25	0.125	0.3013(2)	0.672(1)	0.672(1)	0.91	3.3k
48	48	-0.25	0.123	0.4546(3)	0.976(2)	0.976(2)	0.91	3.5k
48	48	0.001	0.1299	0.0170(1)	0.19(2)	0.16(3)	0.92	2.1k
48	48	0.001	0.129	0.0517(1)	0.173(4)	0.158(4)	0.93	1.3k
48	48	0.001	0.125	0.2179(1)	0.492(1)	0.491(1)	0.92	3.2k
48	48	0.001	0.12	0.5074(3)	1.052(3)	1.053(3)	0.93	3.6k
48	48	0.25	0.129	0.0151(1)	0.18(3)	0.15(3)	0.91	1.9k
48	48	0.25	0.125	0.1658(1)	0.373(1)	0.373(1)	0.93	2.9k
48	48	0.25	0.12	0.3853(1)	0.810(3)	0.810(3)	0.93	3.6k
48	48	0.25	0.115	0.7534(7)	1.42(2)	1.42(2)	0.94	3.4k

Table IX. Same as Table II for $N_t = 48$, $N_s = 48$.

- [24] A. Hasenfratz, C. Rebbi and O. Witzel, Phys. Rev. D **100** (2019) no.11, 114508 doi:[10.1103/PhysRevD.100.114508](https://doi.org/10.1103/PhysRevD.100.114508) [arXiv:[1909.05842](https://arxiv.org/abs/1909.05842) [hep-lat]].
- [25] A. Hasenfratz, C. Rebbi and O. Witzel, Phys. Rev. D **101** (2020) no.11, 114508 doi:[10.1103/PhysRevD.101.114508](https://doi.org/10.1103/PhysRevD.101.114508) [arXiv:[2004.00754](https://arxiv.org/abs/2004.00754) [hep-lat]].
- [26] Y. Shamir, B. Svetitsky and T. DeGrand, Phys. Rev. D **78** (2008), 031502 doi:[10.1103/PhysRevD.78.031502](https://doi.org/10.1103/PhysRevD.78.031502) [arXiv:[0803.1707](https://arxiv.org/abs/0803.1707) [hep-lat]].
- [27] T. DeGrand, Y. Shamir and B. Svetitsky, Phys. Rev. D **79** (2009), 034501 doi:[10.1103/PhysRevD.79.034501](https://doi.org/10.1103/PhysRevD.79.034501) [arXiv:[0812.1427](https://arxiv.org/abs/0812.1427) [hep-lat]].
- [28] Z. Fodor, K. Holland, J. Kuti, D. Nogradi and C. Schroeder, JHEP **11** (2009), 103 doi:[10.1088/1126-6708/2009/11/103](https://doi.org/10.1088/1126-6708/2009/11/103) [arXiv:[0908.2466](https://arxiv.org/abs/0908.2466) [hep-lat]].
- [29] T. DeGrand, Y. Shamir and B. Svetitsky, Phys. Rev. D **82** (2010), 054503 doi:[10.1103/PhysRevD.82.054503](https://doi.org/10.1103/PhysRevD.82.054503) [arXiv:[1006.0707](https://arxiv.org/abs/1006.0707) [hep-lat]].
- [30] Z. Fodor, K. Holland, J. Kuti, S. Mondal, D. Nogradi and C. H. Wong, JHEP **09** (2015), 039 doi:[10.1007/JHEP09\(2015\)039](https://doi.org/10.1007/JHEP09(2015)039) [arXiv:[1506.06599](https://arxiv.org/abs/1506.06599) [hep-lat]].
- [31] T. DeGrand, Y. Shamir and B. Svetitsky, Phys. Rev. D **85** (2012), 074506 doi:[10.1103/PhysRevD.85.074506](https://doi.org/10.1103/PhysRevD.85.074506) [arXiv:[1202.2675](https://arxiv.org/abs/1202.2675) [hep-lat]].
- [32] T. DeGrand, Y. Liu, E. T. Neil, Y. Shamir and B. Svetitsky, Phys. Rev. D **91** (2015), 114502 doi:[10.1103/PhysRevD.91.114502](https://doi.org/10.1103/PhysRevD.91.114502) [arXiv:[1501.05665](https://arxiv.org/abs/1501.05665) [hep-lat]].
- [33] V. Leino, T. Rindlisbacher, K. Rummukainen, F. Sannino and K. Tuominen, Phys. Rev. D **101** (2020) no.7, 074508 doi:[10.1103/PhysRevD.101.074508](https://doi.org/10.1103/PhysRevD.101.074508) [arXiv:[1908.04605](https://arxiv.org/abs/1908.04605) [hep-lat]].
- [34] F. Jegerlehner and O. V. Tarasov, Nucl. Phys. B **549** (1999), 481-498 doi:[10.1016/S0550-3213\(99\)00141-8](https://doi.org/10.1016/S0550-3213(99)00141-8) [arXiv:[hep-ph/9809485](https://arxiv.org/abs/hep-ph/9809485) [hep-ph]].
- [35] S. Capitani, S. Durr and C. Hoelbling, JHEP **11** (2006), 028 doi:[10.1088/1126-6708/2006/11/028](https://doi.org/10.1088/1126-6708/2006/11/028) [arXiv:[hep-lat/0607006](https://arxiv.org/abs/hep-lat/0607006) [hep-lat]].
- [36] R. C. Brower, T. Ivanenko, A. R. Levi and K. N. Orginos, Nucl. Phys. B **484** (1997), 353-374 doi:[10.1016/S0550-3213\(96\)00579-2](https://doi.org/10.1016/S0550-3213(96)00579-2) [arXiv:[hep-lat/9509012](https://arxiv.org/abs/hep-lat/9509012) [hep-lat]].
- [37] A. Hasenfratz and T. A. DeGrand, Phys. Rev. D **49** (1994), 466-473 doi:[10.1103/PhysRevD.49.466](https://doi.org/10.1103/PhysRevD.49.466) [arXiv:[hep-lat/9304001](https://arxiv.org/abs/hep-lat/9304001) [hep-lat]].
- [38] T. Blum, C. E. DeTar, U. M. Heller, L. Karkkainen, K. Rummukainen and D. Toussaint, Nucl. Phys. B **442** (1995), 301-316 doi:[10.1016/0550-3213\(95\)00137-9](https://doi.org/10.1016/0550-3213(95)00137-9) [arXiv:[hep-lat/9412038](https://arxiv.org/abs/hep-lat/9412038) [hep-lat]].
- [39] P. de Forcrand, S. Kim and W. Unger, JHEP **02** (2013), 051 doi:[10.1007/JHEP02\(2013\)051](https://doi.org/10.1007/JHEP02(2013)051) [arXiv:[1208.2148](https://arxiv.org/abs/1208.2148) [hep-lat]].
- [40] B. Bolder, T. Struckmann, G. S. Bali, N. Eicker, T. Lippert, B. Orth, K. Schilling and P. Ueberholz, Phys. Rev. D **63** (2001), 074504 doi:[10.1103/PhysRevD.63.074504](https://doi.org/10.1103/PhysRevD.63.074504) [arXiv:[hep-lat/0005018](https://arxiv.org/abs/hep-lat/0005018) [hep-lat]].